

METAL ENRICHMENT OF THE INTERGALACTIC MEDIUM AT $Z = 3$ BY GALACTIC WINDSANTHONY AGUIRRE,^{a,b} LARS HERNQUIST,^b JOOP SCHAYE,^a DAVID H. WEINBERG,^c NEAL KATZ,^a
& JEFFREY GARDNER^e^aInstitute for Advanced Study, School of Natural Sciences, Princeton NJ 08540^bDepartment of Astronomy, Harvard University 60 Garden Street, Cambridge, MA 02138^cDepartment of Astronomy, Ohio State University, Columbus, OH 43210^dDepartment of Astronomy, University of Massachusetts, Amherst, MA 01003^eDepartment of Astronomy, University of Washington, Seattle, WA 98195*Submitted to the Astrophysical Journal*

ABSTRACT

Studies of quasar absorption lines reveal that the low density intergalactic medium at $z \sim 3$ is enriched to $10^{-3} - 10^{-2}$ solar metallicity. This enrichment may have occurred in an early generation of Population III stars at redshift $z \gtrsim 10$, by protogalaxies at $6 \lesssim z \lesssim 10$, or by larger galaxies at $3 \lesssim z \lesssim 6$. This paper addresses the third possibility by calculating the enrichment of the IGM at $z \gtrsim 3$ by galaxies of baryonic mass $\gtrsim 10^{8.5} M_{\odot}$. We use already completed cosmological simulations to which we add a prescription for chemical evolution and metal ejection by winds, assuming that the winds have properties similar to those observed in local starbursts and Lyman-break galaxies. Results are given for a number of representative models, and we also examine the properties of the galaxies responsible for the enrichment as well as the physical effects responsible for wind escape and propagation. We find that winds of velocity $\gtrsim 200 - 300 \text{ km s}^{-1}$ are capable of enriching the IGM to the mean level observed, though many low-density regions would remain metal free. Calibrated by observations of Lyman-break galaxies, our calculations suggest that most galaxies at $z \gtrsim 3$ should drive winds that can escape and propagate to large radii. The primary effect limiting the enrichment of low-density IGM gas in our scenario is then the travel time from high- to low-density regions, implying that the metallicity of low-density gas is a strong function of redshift.

Subject headings: cosmology: theory — intergalactic medium — galaxies: abundances, starburst

1. INTRODUCTION

The detailed comparison of quasar absorption spectra with the predictions of cosmological hydrodynamic simulations has established that the Ly α absorption ‘forest’ is caused by a smoothly-fluctuating neutral component of the intergalactic medium (IGM) (e.g., Cen et al. 1994; Zhang, Anninos, & Norman 1995; Hernquist et al. 1996). The simulations also reveal a strong correlation between absorber H I column density and gas overdensity $\delta \equiv \rho_{\text{gas}}/\langle \rho_{\text{gas}} \rangle$, so that the study of $N(\text{HI}) \lesssim 10^{15} \text{ cm}^{-2}$ absorbers gives information about the IGM for $\delta \lesssim 10$ at $z \gtrsim 3$ (e.g. Zhang et al. 1998; Davé et al. 1999). Furthermore, studies of CIV, SiIV and OVI have revealed that the low-density IGM is not – as was long expected – chemically pristine, but has been enriched to $\sim 10^{-2.5} Z_{\odot}$ (with a scatter of $\sim 1 \text{ dex}$) down to $N(\text{H I}) \approx 10^{14.5}$ ($\delta \sim 5$) (e.g., Meyer & York 1987; Songaila & Cowie 1996), and perhaps to even lower overdensities (e.g., Cowie & Songaila 1998; Ellison et al. 2000; Schaye et al. 2000).

This enrichment may have occurred during a Population III star-formation epoch at $z \gg 5$ (e.g. Carr, Bond & Arnett 1984; Ostriker & Gnedin 1996; Haiman & Loeb 1997; Abel et al. 1998), later through the disruption of small ‘protogalaxies’ at $6 - 8 \lesssim z \lesssim 10 - 20$ (e.g. Gnedin & Ostriker 1997; Gnedin 1998; Madau, Ferrara & Rees 2001), or even more recently by the ejection of metals from fairly massive galaxies at $z \lesssim 6 - 8$. Earlier enrichment might allow more uniform IGM pollution (depending on

how strongly biased the star formation is), but is constrained by the amount of metal that can be generated at early times; conversely, sufficient metal is easily available at late times, but the larger inter-galaxy spacing may preclude a homogeneous metal distribution (which observations may or may not indicate).

In this paper, we address enrichment of the IGM by supernova-driven winds from galaxies of (gas+star) masses $\gtrsim 10^{8.5}$ at $z \lesssim 8$. Our calculations employ a smoothed-particle hydrodynamics (SPH) simulation with 128^3 dark matter particles and 128^3 SPH particles in a $(17 \text{ Mpc})^3$ box, adopting a cosmology with $\Omega_{\Lambda} = 0.6$, $\Omega_b = 0.047$ and $\Omega_m = \Omega_{\text{CDM}} + \Omega_b = 0.4$. The simulation is described in more detail in Aguirre et al. (2001) and in Weinberg et al. (1999). These simulations do *not* include winds, but we use a parameterized prescription, described in § 2, to add metals in a way that models their ejection and distribution by supernova-driven galactic outflows. This post-processing method allows us to easily vary our assumptions and parameters, and we give results for a number of representative models. We then compare the resulting intergalactic metal distribution to the quasar absorption line observations and discuss the implications for wind enrichment of the IGM.

2. METHOD

The method by which we calculate IGM enrichment is discussed in detail in Aguirre et al. (2001). Briefly, our method employs a limited number of outputs from already

completed SPH simulations that include star formation. Each unit of forming stellar mass instantaneously generates y_* units of metal mass ($y_* = Z_\odot$ is assumed for all models). We then deposit this metal mass in nearby gas particles as follows:

1. Particles are grouped¹ into bound objects ('galaxies'). The mass of star formation is tallied for a given galaxy, for which we also compute the mass, star-formation rate (SFR), and an area $A = 44(M/10^{11} M_\odot)^{0.76}$ kpc² based on an empirical relation between disk area and mass (Gavazzi, Peirini & Boselli 1996).
2. Galaxies with $SFR/A > SFR_{\text{crit}} = 0.1 M_\odot \text{yr}^{-1} \text{kpc}^{-2}$ are assumed to coherently drive steady-state, mass-conserving winds with velocity v_{out} at the center of star formation and with a mass outflow rate of $\dot{m} = 1.3\chi(600 \text{ km s}^{-1}/v_{\text{out}})^2$ times the SFR. Here χ parameterizes the fraction of supernova kinetic energy in the wind, if we assume 10^{51} ergs are released per $100 M_\odot$ of star formation. Based on observations that generally $\dot{m} \sim 1 M_\odot \text{yr}^{-1}$ (Heckman et al. 2000), we use $\chi = 1$. We allow galaxies with $SFR/A < SFR_{\text{crit}}$ to drive winds also, but with the wind energy attenuated by $[(SFR/A)/(SFR_{\text{crit}})]^4$.
3. We divide the volume about the center of star formation into N_a regions of equal solid angle about directions (θ_i, ϕ_i) , with ~ 16 galactic gas particles per region (thus N_a increases with galaxy mass).
4. For each angle (θ_i, ϕ_i) we integrate the equations of motion of a 'test shell' beginning at radius r_0 containing 10% of the galaxy's mass. The shell at radius r feels accelerations due to gravity, the ram pressure of the wind (attenuated by the potential difference between r and r_0), the ambient thermal pressure, and the sweeping up of a fraction ϵ_{ent} of the ambient medium (matter could be left behind by the shell either if the ambient medium is inhomogeneous, or as the shell fragments and leaves part of itself with lower velocity. We take a fiducial value of $\epsilon_{\text{ent}} = 0.1$). All accelerations are computed using the simulation particles contained in the solid angle about (θ_i, ϕ_i) (see Aguirre et al. 2001 for details). Eventually, the shell stalls (i.e. has a negligible velocity with respect to the local medium) at a radius $r_{\text{stall}}(\theta, \phi)$. We also stop the shell if/when its propagation time exceeds the time between its launch and the redshift at which we quote our results.
5. In each angular region, metals are distributed among gas particles within $r_{\text{stall}}(\theta, \phi)$ such that the metal mass in a shell at r of thickness dr is $\propto (r/r_{\text{stall}})^\alpha dr$. We generally take $\alpha = 3$, but the resulting enrichment is rather insensitive to α for $2 \lesssim \alpha \lesssim 5$ (Aguirre et al. 2001).
6. If $r_{\text{stall}} < 2r_0$ for some angle, the corresponding metal mass is not distributed as per the wind prescription, but is deposited 'locally' over the 32 gas

particles nearest to its progenitor star, using the SPH smoothing kernel (see, e.g., Hernquist & Katz 1989).

The process is repeated for each galaxy, at each time step. New stars are formed with the metallicity of the gas from which they form. Metals accumulate in gas particles (which move between time steps), and the distribution of metals in stars and in galactic and intergalactic gas can be assessed at each time step.

3. RESULTS

3.1. Enrichment of the IGM

We first give results for six illustrative models. The first four have all their parameters fixed (to the 'fiducial' values given above) except for the wind outflow velocity v_{out} , which we take to be $600 \pm 200 \text{ km s}^{-1}$, $300 \pm 200 \text{ km s}^{-1}$, $200 \pm 100 \text{ km s}^{-1}$, or $100 \pm 50 \text{ km s}^{-1}$ (uniformly distributed in the given range for each model), independent of galaxy mass (as suggested by Heckman et al. 2000). Next, we fix $v_{\text{out}} = 300 \pm 200 \text{ km s}^{-1}$ and vary the entrainment fraction ϵ_{ent} from 1% to 100%.

The key results of the calculations are shown in Fig. 1. The top two panels give a sparse sampling of individual particle metallicities, versus the gas overdensity δ . The stellar yield y_* is uncertain by perhaps a factor of two, and all of the curves could be scaled vertically for a higher assumed value.² The metallicity at $\delta \lesssim 10^4$ could also be (roughly) scaled down by a factor $(1 - Y_{\text{ret}})$ if a fraction Y_{ret} of the metal produced is assumed not to be incorporated into the wind. Panel A shows that in the 600 km s^{-1} model, the enrichment is fairly uniform. A significant fraction of particles (shown in a bar at the bottom with an artificial 1 dex of scatter added) have zero metallicity, but the rest have a metallicity spread at a given overdensity of $\sim 1\text{-}2$ dex. In contrast, the 300 km s^{-1} model (panel B) has *some* metal rich particles at low densities, but many more pristine regions that the winds have not reached.

Panels C and D show the median and mean gas metallicities vs. overdensity for all six models. The shaded box indicates the rough range of metallicity found in most absorption systems for which metal lines are detected. The area with vertical lines indicates the region where the metallicity is agreed upon by independent groups (e.g., Rauch, Haehnelt, & Steinmetz 1997; Davé et al. 1998). The horizontal lines indicate yet smaller overdensities to which this metallicity may extend (e.g., Ellison et al. 2000; Schaye et al. 2000). Even if the observational results were complete, neither the mean nor the median particle metallicities we quote are directly comparable to the observational results, but should bracket the quantity that is comparable. The mean would be too high because (especially in cases with inhomogeneous distributions) it tends to be dominated by a small number of high-metallicity regions; the median gives information about the *number* of lines that would be metal rich, but is an underestimate because an absorption line would generally probe more than one simulation gas particle, decreasing the scatter.

¹The grouping is done using the SKID package, publicly available at <http://www-hpcc.astro.washington.edu/tools>.

²The yield can be constrained using the metallicities of observed galaxies; see Aguirre et al. (2001).

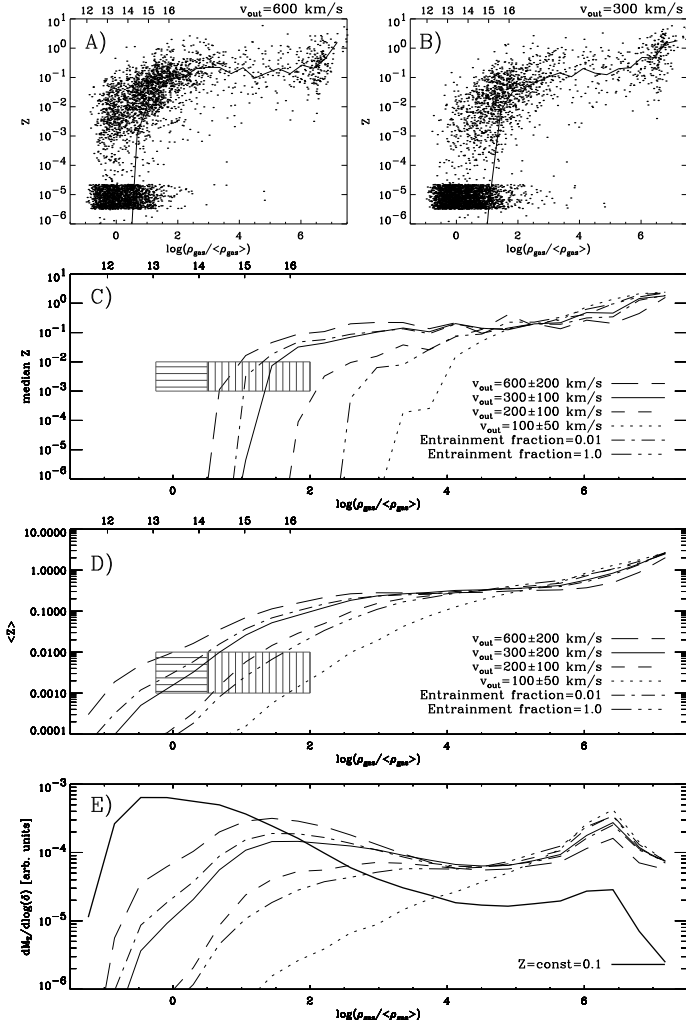


FIG. 1.— Enrichment of the IGM at $z = 3$ as a function of gas density. **A:** Random subsample (1 in 500) of particle metallicities for wind model with $v_{\text{out}} = 600 \text{ km s}^{-1}$, versus over-density $\delta \equiv \rho_{\text{gas}}/\langle \rho_{\text{gas}} \rangle$. Top axis (here and in all panels) gives approximate $\log N(HI)$, using the relation of Schaye (2001; assuming his fiducial parameters). The solid line shows the median metallicity versus δ . **B:** As for panel A, but in a $v_{\text{out}} = 300 \text{ km s}^{-1}$ model. **C:** Median metallicity versus δ for wind models with $v_{\text{out}} = 100, 200, 300, 600 \text{ km s}^{-1}$, and for ‘minimal’ and ‘maximal’ outflow models (as described in text). The shaded box roughly indicates the metallicity of low-column density Ly α clouds. **D:** As for panel C, but *mean* metallicity are plotted. **E:** As for panel C, but gives mean metallicity times the fraction of baryons at a given δ , showing the contribution by components with different δ to the cosmic metal density. The thick solid line shows the distribution assuming constant metallicity (with the same total metal mass).

In panel E the gas metallicity is multiplied by the fraction of gas at the given overdensity, showing what fraction of all cosmic metal lies at a given density. For the models that can plausibly account for the observed metal lines in the IGM, $\sim 10 - 30\%$ of all metal is extragalactic (EG), i.e. is not in cooled gas or stars in galaxies.

The curves show that the assumed wind velocity at inception is quite important in the resulting IGM enrichment. Slow winds tend to be confined, as can be seen from the small fraction (2%) of all metals outside of galaxies in the 100 km s^{-1} model (see panel E). Those that escape tend to stall at relatively small distances where

the density is still high, and fail to effectively pollute the low-density IGM. Increasing v_{out} both increases the total EG metal density (raising the EG fraction to 50% for $v_{\text{out}} = 600 \text{ km s}^{-1}$) and shifts the metals to lower density regions (increasing the $\delta = 1$ mean enrichment by a factor of several hundred). Changes in the entrainment fraction also have a fairly large effect. If (instead of the fiducial 10%) only 1% of the ambient gas were entrained, 20% of all metals would be outside of galaxies in our fiducial 300 km s^{-1} model; while only 4% would be extragalactic if all ambient gas were entrained. Changing our other model parameters within a range of reasonable values has a smaller but still substantial effect; doubling SFR_{crit} or changing χ by a factor of two changes the ejection fraction by $\lesssim 30\%$ and changes the mean enrichment at $\delta = 1$ by $\lesssim 50\%$ (Lowering SFR_{crit} would have little effect since most galaxies at $z > 3$ are already driving winds for our assumed value.)

Two methodological points concerning our results merit discussion. First, resolution tests reveal that galaxies with $\gtrsim 6 \times 10^8 M_{\odot}$ in baryons are well-resolved. Galaxies below this limit exist (and are used in the analysis) but will be under-represented both in their number and in their star-formation rates (Weinberg et al. 1999). Studies of dwarf galaxies at high z have concluded that at $z \lesssim 6$, galaxies of baryon mass $\lesssim 5 \times 10^7 M_{\odot}$ are suppressed by photo-evaporation (e.g., Ferrara & Tolstoy 1999), leaving a (redshift-dependent) ‘gap’ in mass where galaxies may exist but are not resolved by our simulations.

Second, our method necessarily neglects the effect of the outflows on the galaxies. Galaxy formation studies with ineffective feedback generally predict more low-mass galaxies than are observed, and the simulations used here may over-estimate the cosmic SFR and stellar mass for this reason (see Weinberg et al. 1999 and Aguirre et al. 2001). While we cannot quantify exactly the effect these two (opposing) inaccuracies will have on our results, comparison of the mass functions for different numerical resolutions indicates that we can probably hope to estimate the enrichment by $z \lesssim 6$ galaxies to within a factor of a few.³

Because IGM enrichment is so sensitive to v_{out} , we can set a lower limit on that quantity if the observed enrichment is primarily due to winds of the type discussed in this paper. To achieve the *mean* metallicity of $10^{-2.5} Z_{\odot}$ observed in $N(\text{HI}) \sim 10^{14.5}$ absorbers, $v_{\text{out}} \gtrsim 200 \text{ km s}^{-1}$ is necessary, and $v_{\text{out}} \gtrsim 300 \text{ km s}^{-1}$ would be needed to enrich absorbers down to $N(\text{HI}) \sim 10^{13.5}$ with a similar metallicity (though this may *over-enrich* higher column density systems). A higher velocity is probably necessary if the observed enrichment is fairly uniform; for a *median* metallicity of $\sim 10^{-2.5} Z_{\odot}$ down to $N(\text{HI}) \sim 10^{14.5} \text{ cm}^{-2}$, a wind speed of $v_{\text{out}} \gtrsim 300 \text{ km s}^{-1}$ is probably required, though a more detailed analysis is necessary for a robust comparison. These conclusions depend on the assumed entrainment fraction (and more weakly on the other parameters), but changing these assumptions cannot increase the enrichment very much because enrichment is always limited by the available time between shell launch and $z = 3$. Thus if the observed enrichment turns out to be uniform at

³This assumes that the missing low-mass galaxies are distributed like the higher-mass galaxies. If low mass galaxies are strongly biased toward appearing in low-density regions, then the results may differ significantly when they are included.

column densities $N(\text{H I}) \ll 10^{14.5} \text{ cm}^{-2}$, enrichment from smaller and/or higher redshift galaxies would be required.

3.2. Physics of outflows

In addition to providing estimates of intergalactic enrichment, our calculations also shed light on the physics of wind escape. Figure 2 gives information about the outflows propagating between $z \approx 4$ and $z = 3$ from individual galaxies in the $v_{\text{out}} = 300 \text{ km s}^{-1}$ model. Panel A shows the shell stalling radius for each shell about a sample of 500 simulation galaxies; each point corresponds to one propagation direction and each vertical ‘stripe’ to a galaxy. At $3 \leq z \lesssim 4$ about half of all galaxies are driving winds that reach $r_{\text{stall}} \gg 10 \text{ kpc}$. The variation in r_{stall} for a given galaxy is due to anisotropies in the galaxy and IGM; variations in r_{stall} among galaxies of a given mass are due to combined variations in the outflow velocity, the SFR and the properties of the nearby IGM. Since we have assumed that wind velocity is independent of galaxy mass, the most massive galaxies drive winds ineffectively because of their relatively large potential wells. The cutoff at $r_{\text{stall}} \sim 100 \text{ kpc}$ is due to the finite time between $z \sim 4$ and $z = 3$ (where we stop each shell’s integration). This is shown in Panel B, which displays the stalling time for the shell segments (one point for each angle). As shown in Panel C, at $z = 4$ almost all of the galaxies exceed the assumed critical SFR/(area). But as long as this threshold is satisfied, the areal SFR does not strongly influence how well winds escape.

Panel D allows a comparison of our results for wind escape with two other investigations. The points in the figure indicate the supernova energy injection rate for each galaxy in units of 10^{38} ergs , converted from star formation rates by assuming that one supernova releasing $10^{51} E_{51} \text{ ergs}$ forms per per $100 M_{100} M_{\odot}$ of star formation. The vertically shaded region indicates the range of SFRs measured in bright, wind-driving Lyman-break galaxies by Pettini et al. (2001), converted in the same way. The solid line is a fit that extrapolates the simulation results to lower-mass galaxies, and the dotted line represents our fiducial critical SFR/area (i.e. we assume that galaxies above the dotted line are driving winds coherently – though the winds may ultimately be retained as shown in panel A). Mac Low & Ferrara (1999; see also Ferrara & Tolstoy 2000) have studied galactic winds in dwarf galaxies using numerical simulations, for the range of galaxy masses and supernova energy injection rates shown by the shaded box. They find that only the lowest-mass galaxies ($10^6 M_{\odot}$) can ‘blow-away’ the bulk of their ISM, though higher mass galaxies can allow ‘blowout’ where hot, metal rich gas can escape. Their results agree roughly with the estimates of Silich & Tenorio-Tagle (2001), who find that winds can only escape spherical galaxies (corresponding to ‘blowout’) for energy injection rates above the dashed line of Panel D; winds can escape flattened galaxies for rates above the dot-dashed line. According to our calculations, winds can escape the simulation galaxies (which are not highly flattened), even for entrainment fraction unity, from galaxies with mass $\gg 10^6 M_{\odot}$. This would seem to conflict with the findings of Mac Low & Ferrara (1999), but the disagreement is probably due to the rather small energy injection rates they assume for their largest galaxies – 10^4

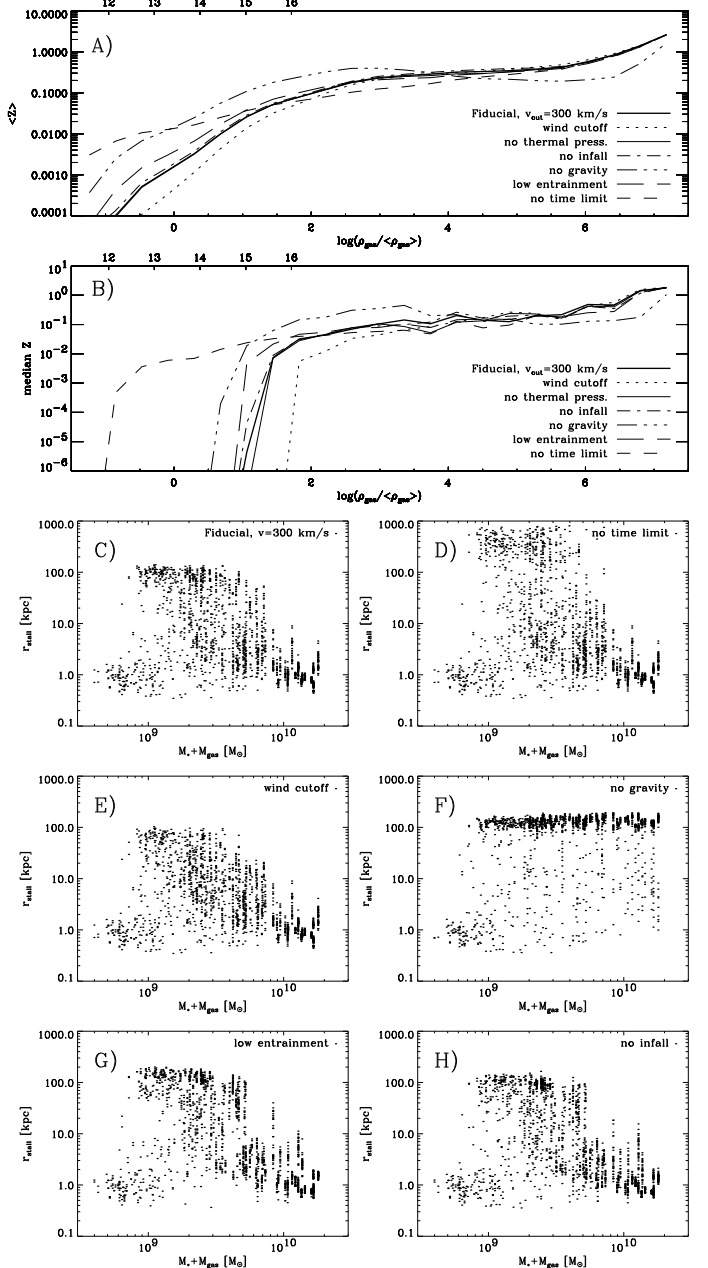


FIG. 3.— Enrichment of the IGM at $z = 3$ for the fiducial model with $v = 300 \text{ km s}^{-1}$, with various effects turned off. **A:** Mean metallicity versus δ for wind models with gravity, wind ram pressure, IGM thermal pressure, IGM infall, or the time limit turned off. **B:** As in panel A, but median metallicity. **C-F:** Wind stalling radius for wind propagating between $z = 4$ and $z = 3$, versus galaxy baryon mass, with various effects turned off (see text).

times smaller than the rate indicated by the cosmological simulations. The simulated galaxy SFRs at high z are high enough to fulfill the (extrapolated) ‘blow-away’ criterion of Silich & Tenorio-Tagle for all galaxy masses, as are the SFRs of the Lyman-break galaxies (unless the galaxies have masses $\gtrsim 10^{11} M_{\odot}$).

In Figure 3 we show plots of both IGM enrichment and stalling radius vs. mass in the fiducial model with each effect on shell propagation turned off in turn. First (panel D) we remove the time constraint. This shows that some shell fragments from $z = 4$ galaxies would ultimately

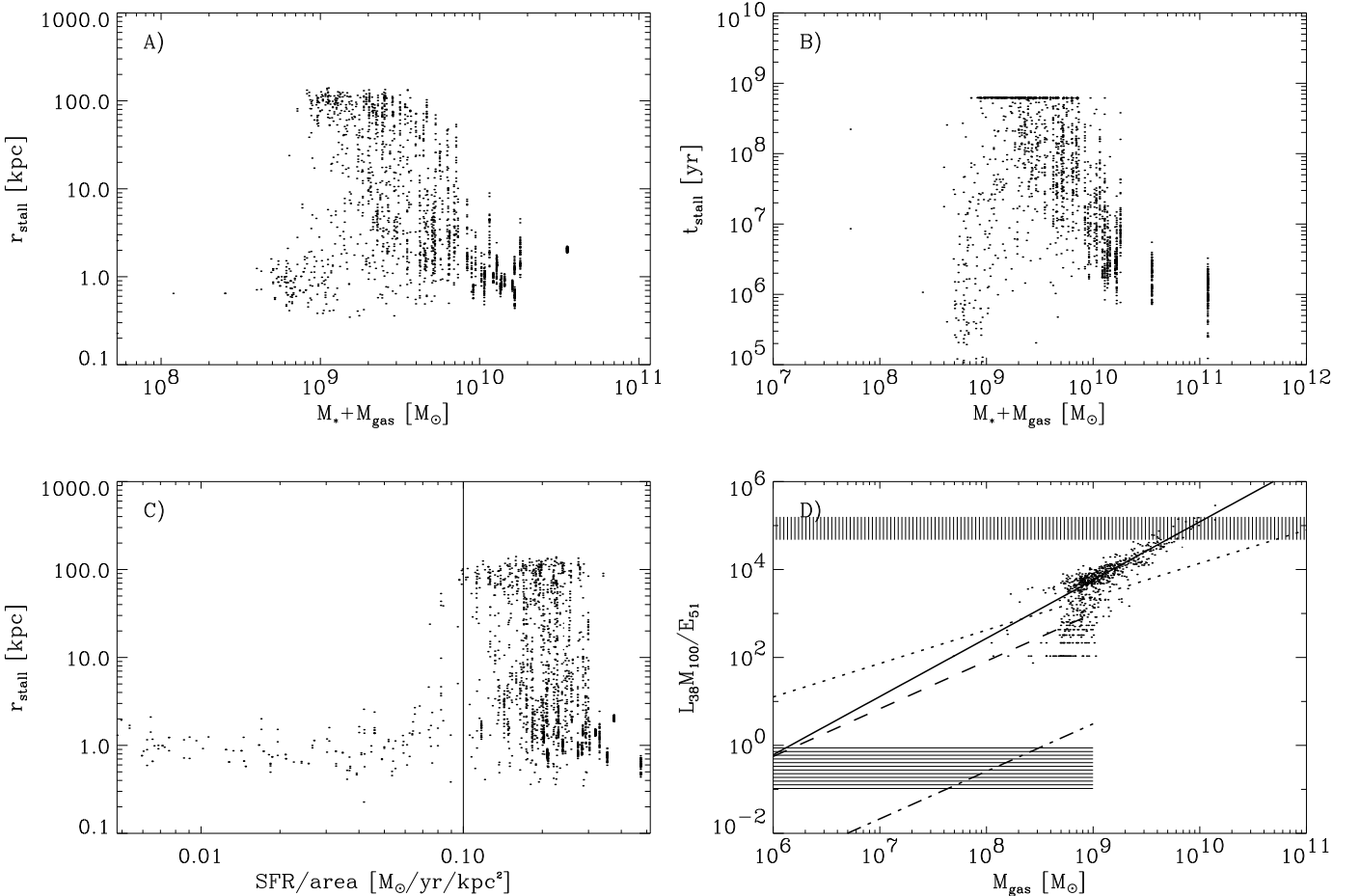


FIG. 2.— Quantities at $z = 4$ for wind-driving galaxies. **Panel A:** Wind stopping radius r_{stall} (i.e. where the shell has small velocity w.r.t. the ambient medium or runs out of time at $z = 3$) versus galactic baryonic mass. **Panel B:** Time between shell launch at $z = 4$ and stalling; the strip just below 10^9 yr corresponds to the time between $z = 4$ and $z = 3$. **C:** r_{stall} vs. total SFR/area of galaxy. **D:** Supernova energy generation rate in units of $10^{38} \text{ erg s}^{-1}$ versus galactic baryonic mass, assuming $10^{51} E_{51}$ ergs per supernova and 1 supernova per $100 M_{100} M_{\odot}$ of star formation. Points show the simulated galaxies, to which the solid line is fit. The dotted line corresponds to our fiducial value of SFR_{crit} . The upper (vertically) shaded region is the range of SFRs ($10 - 50 M_{\odot}/\text{yr}$) found by Pettini et al. (2001) converted in the same manner. The lower shaded region is the parameter space probed by Mac Low & Ferrara (1999). The dashed and dot-dashed lines are the critical luminosities derived by Silich & Tenorio-Tagle (2001) for wind escape from spherical and disk galaxies, respectively.

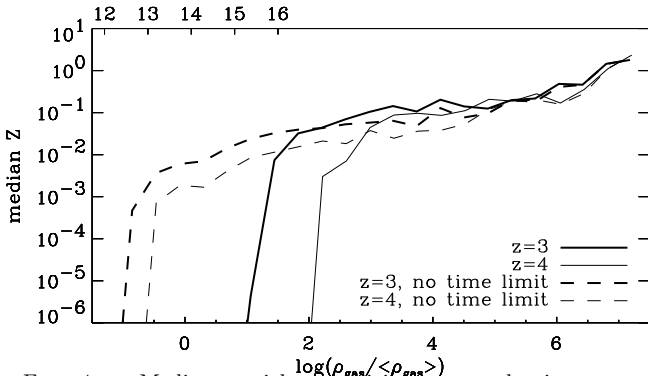


FIG. 4.— Median particle metallicity vs. overdensity at $z = 3$ and $z = 4$, with or without wind propagation stopped at the given redshift.

propagate to ~ 1 Mpc (the cutoff comes from the distance d at which $Hd = v_{\text{out}}$). Panel E shows the results if the wind is turned off 10^8 years after the shell launch. This is roughly the minimal interval τ_d over which a starburst ‘event’ could drive the shell, since the energy deposition rate is roughly constant for $\tau_e \sim 4 \times 10^7$ yr after a coeval starburst (Tenorio-Tagle et al. 1999), and the wind (or thermal pressure) will still drive the shell for the time τ_c it takes the wind (or sound) to cross the shell radius. If the shell speed is comparable to the wind speed, $\tau_e \sim \tau_c$ so $\tau_d \sim 2\tau_e$. The effect of truncating the wind is noticeable but slight. In panel F we have turned off gravity, and essentially all of the shells escape, showing that in this case gravity is the dominant effect in confining winds. Of the shells that still do not escape, about half are retained due to thermal pressure, and about half due to the sweeping up of matter. Panel G shows the effect of very low mass entrainment: winds escape to slightly larger radii on average, but can actually increase the escape radius in some cases because higher entrainment adds more momentum to the shell. Entrainment actually causes as much deceleration on the shell as gravity; but since gravity also attenuates the wind (decreasing the acceleration of the shell), it has a larger overall effect. Panel H shows that taking into account infall from the IGM is not very important, but tends to slightly decrease the stalling radius. In summary, we find that only the hot wind, the entrainment of ambient material and gravity are important in determining shell propagation in most cases at $z = 3$. More hot gas (especially in clusters) and stronger infall, however, might make thermal pressure and IG infall more important at low z .

The most important factor limiting the enrichment of very low density regions is the time constraint as shown in Fig. 4. If we assume that the winds can propagate ‘instantaneously’ into the IGM, they reach quite low-density regions, and the enrichment at $z = 3$ is only slightly higher and more uniform than at $z = 4$. But if the time limit is respected, the enrichment spreads to significantly lower-density regions between $z = 4$ and $z = 3$ due to the extra Gyr of propagation time.

4. DISCUSSION AND IMPLICATIONS

Metal enrichment of the $z \sim 3$ IGM has also been investigated by Gnedin & Ostriker (1997), Gnedin (1998) and Cen & Ostriker (1999) using simulations that include

chemical evolution. Gnedin finds that supernova blow-apart of protogalaxies is ineffective, but that dynamical removal of metals can explain the metals in low-density regions – though this requires a metal formation rate at $z \gtrsim 4$ that is about 10-50 times that observationally inferred at $z \sim 3 - 4$ (e.g., Steidel et al. 1999) and implies more efficient dynamical removal of metals than found by Aguirre et al. (2001).

Cen & Ostriker (1999) assume a fixed metal ejection fraction into regions of ~ 400 kpc (the resolution of their grid-based hydrodynamical treatment; see Cen & Ostriker 2000). Their results for mean metallicity are similar to our $v = 200$ km s $^{-1}$ model, though their metallicity distribution at fixed δ shows almost no scatter at $z = 3$ (but becomes more inhomogeneous with time). In contrast, our calculations find a highly inhomogeneous metallicity distribution, which becomes somewhat more uniform with time. This may be due to the rather low spatial resolution of their simulations or may indicate that stars are forming (and expelling metals into the IGM) in very low density regions in Cen & Ostriker’s simulations, in contrast to ours. Comparison of quasar absorption spectra to simulated spectra shows that ~ 0.5 dex of scatter in gas metallicity (among absorbers in which metals are detected) may be necessary to explain the variation in observed CIV/HI ratios (Rauch et al. 1997; Hellsten et al. 1997; Davé et al. 1998), so this point merits further investigation, but will probably require the generation of synthetic spectra from our simulations.

An important physical effect that is not addressed by our treatment is that of the outflowing winds on the IGM: if metals are transported directly from galaxies to very low density regions by movement of large quantities of gas, then this kinetic energy must be absorbed by the IGM. Yet the widths of low-column density Ly α forest lines are typically $20 - 30$ km s $^{-1}$, and line ratios indicate photoionization, not collisional ionization (e.g. Songaila & Cowie 1996). Our method does not allow us to assess the effects of winds on the IGM (see Theuns, Mo & Schaye [2000] for some discussion), but we can make some general comments. If expanding shells of swept-up gas maintained their integrity and propagated to roughly the inter-galaxy spacing, they would completely re-make the structure of the Ly α forest, except perhaps in deep voids. But this is not the expected scenario: upon leaving a galaxy, the wind and ‘shell’ will likely mix into a complex, multi-phase outflow consisting of fragmented shell(s), the hot wind, dense clouds of entrained (but not swept-up) ambient medium, etc. Small, dense blobs might maintain fairly low temperature through efficient cooling, and could reach large radii before stalling and mixing with the IGM (and by definition when the wind stalls it has small local velocity and will not greatly heat the medium). In addition, the hot wind itself will not be observable in absorption, and will flow more easily in low-density directions. Hence it may not seriously disrupt the relatively dense filaments that give rise to much of the Ly α absorption.

These issues merit further study because our results, combined with observations of high- z galaxies, indicate that significant outflow from $z \gtrsim 3$ galaxies seems inevitable. Essentially all of the simulated galaxies at $z \gtrsim 3$

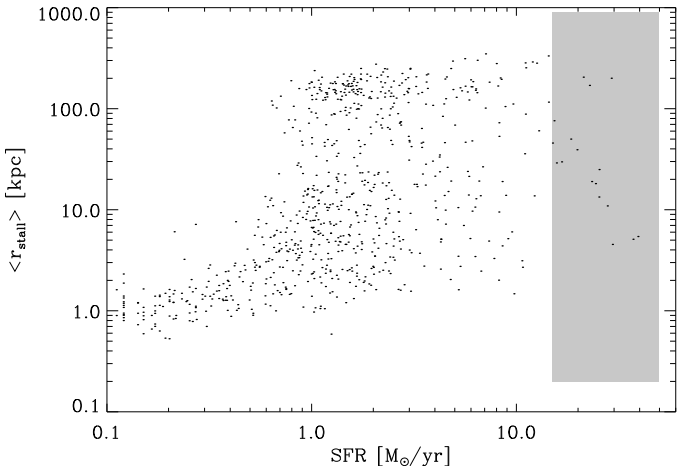


FIG. 5.— Maximum stalling radius in each galaxy vs. star formation rate, at $z = 4$, for $v_{\text{out}} = 750 \pm 500 \text{ km s}^{-1}$ and entrainment fraction unity. The Lyman-break galaxies of Pettini et al. (2001) show SFRs of $10 - 50 \text{ M}_\odot \text{ yr}^{-1}$.

display specific time-averaged SFRs exceeding the observed threshold for driving superwinds in local (starburst) galaxies – and stochastic star formation should result in much higher rates for short periods. Moreover, available observations of $z \sim 3$ galaxies reveal that they *are* driving winds, with characteristic velocities exceeding those of our fiducial model: Pettini et al. (2001) find that Lyman-break galaxies at $z \sim 3$ with SFRs of $\sim 10 - 50 \text{ M}_\odot \text{ yr}^{-1}$ drive winds at $\sim 100 - 800 \text{ km s}^{-1}$ (as measured by absorption lines) or $\sim 250 - 1250 \text{ km s}^{-1}$ (in Ly α emission). These galaxies correspond to the highest ($\sim 10^{10} \text{ M}_\odot$) mass simulated galaxies (see Fig. 2 and Davé et al. 1999). The outflow signatures in the spectra are quite similar to those in the nearby wind-driving starbursts upon which we base our method, so the observed velocities should roughly correspond to our assumed initial outflow velocities. In this case, as shown in Fig. 5, the outflows tend to escape the galaxies even for an entrainment fraction unity, and propagate to large distances – none of the forces we include in our calculations would be capable of containing the outflow. Thus we predict that winds from Lyman-break galaxies do escape those galaxies’ potentials and enrich the IGM,⁴ and expect that this would hold for lower mass galaxies as well.

5. CONCLUSIONS

We have simulated the enrichment of the $z = 3$ IGM by galactic winds from $\gtrsim 10^{8.5} \text{ M}_\odot$ galaxies, assuming that most drive winds with properties similar to those observed in local starbursts and in Lyman-break galaxies. We find that for winds with outflow velocity $v_{\text{out}} \gtrsim 100 \text{ km s}^{-1}$ enrichment is significant, and that if $v_{\text{out}} \gtrsim 300 \text{ km s}^{-1}$, the winds can (roughly) account for the metallicity of the low-column density ($N(\text{H I}) \sim 10^{14.5} \text{ cm}^{-2}$) Ly α forest. Higher velocities could enrich yet lower-density components of the IGM.

Our treatment of wind-driven outflows includes forces due to gravity, thermal pressure, ram pressure of the am-

bient medium, and the hot wind itself. We find that at $z \sim 3$ thermal pressure and the the infall velocity of the IGM are generally negligible, but that outflows can be confined by gravity or ambient material for sufficiently high mass galaxies and/or low velocity winds. Our results suggest that the winds observed in Lyman break galaxies should escape and travel to fairly large distances. If the Lyman break galaxies represent high-mass, non-starburst galaxies, then the lower-mass $z = 3$ galaxies should drive outflows to large distances as well, unless outflow velocity depends strongly on galaxy mass. The effect of such winds on the physical and thermal structure of the IGM is essentially unknown. The good agreement between simulations like these and the observed statistical properties of the Ly α forest suggest that the effect cannot be extremely large.

We find that the main effect preventing the enrichment of very low-density regions of the IGM is the time available for metal-rich material to propagate from galaxies (which are concentrated in filaments) into the voids. This leads to a picture in which a given set of galaxies enriches a progressively larger cosmic volume with decreasing redshift, and we predict that if low-density regions are enriched by winds from $\gtrsim 10^{8.5} \text{ M}_\odot$ galaxies at $z \lesssim 6$, the median metallicity of low-density regions should be a very strong function of redshift.

The scenario described here, enrichment of the IGM by massive ($\gtrsim 10^{8.5} \text{ M}_\odot$) galaxies at modest ($z \lesssim 6$) redshift, is but one of several interpretations for the origin of metal in the Ly α forest. Other possibilities, distinguished by epoch and mass scale, include enrichment by population III stars at $z \sim 20$, or the disruption of low-mass protogalaxies at $z \sim 10$. How are we to decide which, if any, of these three scenarios is most relevant to the real Universe?

Based on our modeling, we anticipate that these mechanisms will predict differences in the metal distribution of the IGM that can be tested observationally. In addition to the mean enrichment, the dispersion in metallicity at a given overdensity and the trend of metallicity with overdensity can both be measured. It seems natural to expect that metal deposition at relatively higher redshift will lead to a rather different distribution of metals than that inferred from our analysis. Thus, future modeling, combined with observational samples of increasingly large size, may discriminate between the various scenarios. To the extent that this goal can be realized, the metals discovered in the $z \sim 3$ Ly α forest may provide a direct probe of the conditions responsible for the production of the first metals in the Universe.

We thank T. Heckman for useful comments and information on superwinds. This work was supported by NASA Astrophysical Theory Grants NAG5-3922, NAG5-3820, and NAG5-3111, by NASA Long-Term Space Astrophysics Grant NAG5-3525, and by the NSF under grants ASC93-18185, ACI96-19019, and AST-9802568. JG was supported by NASA Grant NGT5-50078 for the duration of this work, and AA was supported in part by the National Science Foundation grant no. PHY-9507695 and by a grant in aid from the W.M. Keck Foundation. The sim-

⁴If the Lyman break galaxies actually represent lower-mass, very strongly star-bursting galaxies this conclusion is only strengthened, though it may then be less applicable to the rest of the $z \sim 3$ population.

ulations were performed at the San Diego Supercomputer

Center.

REFERENCES

Aguirre, A. N., Hernquist, L., Schaye, J., D.H., Katz, Weinberg, D.H., & Gardner, J. 2001, ApJ, submitted; astro-ph/0105065

Abel, T., Anninos, P., Norman, M. L. & Zhang, Y. 1998, ApJ, 508, 518

Carr, B. J., Bond, J. R. & Arnett, W. D. 1984, ApJ, 277, 445

Cen, R., Miralda-Escude, J., Ostriker, J. P. and Rauch, M. 1994, ApJ, 437, L9

Cen, R. & Ostriker, J. P. 1999, ApJ, 519, L109

Cen, R. & Ostriker, J. P. 2000, ApJ, 538, 83

Cowie, L. L. & Songaila, A. 1998, Nature, 394, 44

Davé, R., Hellsten, U., Hernquist, L., Katz, N. and Weinberg, D. H. 1998, ApJ, 509, 661

Davé, R., Hernquist, L., Katz, N., & Weinberg, D. 1999, ApJ, 511, 521

Ellison, S., Songaila, A., Schaye, J., & Pettini, M. 2000, AJ, 120, 1175

Ferrara, A. & Tolstoy, E. 2000, MNRAS, 313, 291

Gavazzi, G., Pierini, D. & Boselli, A. 1996, A&A, 312, 397

Gnedin, N. Y. & Ostriker, J. P. 1997, ApJ, 486, 581

Gnedin, N. Y. 1998, MNRAS, 294, 407

Haiman, Z. & Loeb, A. 1997, ApJ, 483, 21

Heckman, T. M., Lehnert, M. D., Strickland, D. K., & Armus, L. 2000, ApJS, 129, 493

Hellsten, U., Davé, R., Hernquist, L., Weinberg, D. H., & Katz, N. 1997, ApJ, 487, 482

Hernquist, L. & Katz, N. 1989, ApJS, 70, 419

Hernquist, L., Katz, N., Weinberg, D. H., & Miralda-Escude, J. 1996, ApJ, 457, L51

Mac Low, M. & Ferrara, A. 1999, ApJ, 513, 142

Mac Low, M. & Ferrara, A., & Rees, M. 2001, ApJ, in press; astro-ph/0010158

Meyer, D. M., & York, D.G. 1987, ApJ, 315, L5

Ostriker, J. P. & Gnedin, N. Y. 1996, ApJ, 472, L63

Pettini, M., Shapley, A., Steidel, C. C., Cuby, J.-G., Dickinson, M., Moorwood, A.F.M., Adelberger, K. L., Dickinson, M., & Giavalisco, M. 2001, ApJ, in press; astro-ph/0102456

Rauch, M., Haehnelt, M. G., & Steinmetz, M. 1997, ApJ, 481, 601

Schaye, J. 2001, ApJ, in press; astro-ph/0104272

Schaye, J., Rauch, M., Sargent, W. L. W., & Kim, T. 2000, ApJ, 541, L1

Silich, S., & Tenorio-Tagle, G. 2001, ApJ, in press; astro-ph/0101317

Songaila, A. & Cowie, L. L. 1996, AJ, 112, 335

Steidel, C. C., Adelberger, K. L., Giavalisco, M., Dickinson, M. & Pettini, M. 1999, ApJ, 519, 1

Tenorio-Tagle, G., Silich, S. A., Kunth, D., Terlevich, E., & Terlevich, R. 1999, MNRAS, 309, 332

Theuns, T., Mo, H.J., & Schaye, J. 2000 MNRAS, 321, 450

Weinberg, D. H., Davé, R., Gardner, J. P., Hernquist, L., & Katz, N. 1999, in Photometric Redshifts and High Redshift Galaxies, eds. R. Weymann, L. Storrie-Lombard, M. Sawicki, & R. Brunner, ASP Conference Series 191, San Francisco, p. 341; astro-ph/9908133

Zhang, Y., Anninos, P. and Norman, M. L. 1995, ApJ, 453, L57

Zhang, Y., Meiksin, A., Anninos, P., & Norman, M. L. 1998, ApJ, 495, 63